Redox Biology 41 (2021) 101890

Contents lists available at ScienceDirect

Redox Biology

journal homepage: www.elsevier.com/locate/redox

Endothelial specific deletion of HMGB1 increases blood pressure and retards ischemia recovery through eNOS and ROS pathway in mice☆

Qin Zhou, Tao Tu, Shi Tai, Liang Tang, Hui Yang, Zhaowei Zhu *

Cardiovascular Department, The Second Xiangya Hospital, Central South University, Changsha, Hunan, China

ARTICLE INFO

Keywords:
HMGB1
Endothelium dependent relaxation
Angiogenesis
Ischemia
Reactive oxygen species
eNOS

ABSTRACT

Recent studies demonstrated HMGB1, an extracellular inflammation molecule, played an important role on endothelial cells. This study aimed to define the role and related mechanism of HMGB1 in endothelial cells. Endothelial-specific deletion of HMGB1(HMGB1ECKO) was generated and Akt/eNOS signaling, reactive oxygen species (ROS) production, endothelium dependent relaxation (EDR), and angiogenesis were determined in vitro and in vivo. Decreased activation of Akt/eNOS signaling, sprouting, and proliferation, and increased ROS production were evidenced in endothelial cells derived from HMGB1ECKO mice as compared with wild type controls. Decreased EDR and retarded blood flow recovery after hind limb ischemia were also demonstrated in HMGB1ECKO mice. Both impaired EDR and angiogenesis could be partly rescued by superoxide dismutase in HMGB1ECKO mice. In conclusion, intracellular HMGB1 might be a key regulator of endothelial Akt/eNOS pathway and ROS production, thus plays an important role in EDR regulation and angiogenesis.

1. Introduction

High-mobility group box 1 protein (HMGB1) is an evolutionarily conserved non-histone nuclear protein, which presents in almost all eukaryotic cells [1]. It can be released to extracellular space post stressful stimulations, and then acts as an extracellular damage associated molecular pattern molecule (DAMP) during cell differentiation or proliferation, inflammation, tissue regeneration, and tumor development [2–4]. Although the function of intracellular HMGB1 in pancreatic cells, hepatocyte, myeloid cells or epithelial cells have been recognized [5–8], its role within the endothelial cells (ECs) or vascular system is still not fully understood.

Endothelium play critical roles in varies homeostatic functions [9]. In general, the vascular endothelium presents some specific functions such as regulating fluid and molecule traffic between blood and tissues, keeping vascular tone and blood flow, anti-coagulation, vascular homeostasis and repairment. Endothelial dysfunction can contribute to the development of atherosclerosis, thrombosis, and relevant complications such as aneurysm, dissection and coronary artery disease [10,11].

The most important feature of endothelial dysfunction is the loss of nitric oxide (NO). The loss of NO in endothelial cells are usually caused by reduced synthesis or activity of endothelial nitric oxide synthase (eNOS) and/or increased scavenging by reactive oxygen species (ROS) [12]. eNOS can be activated mainly by phosphorylation of Ser1177 in human (Ser1176 in mouse) [13]. Although several kinases like Akt, AMPK can phosphorylate eNOS at Ser1177 in vitro, Akt is the only kinase which can regulate eNOS function in vivo. Previous study found that Akt1−/− mice had severe impaired postnatal angiogenesis characteristic. In the condition of fluid shear stress, phosphorylation of eNOS by Akt represents the most important pathway for eNOS activation [14,15].

So far, researchers have indicated an emerging role of HMGB1 in endothelial cells [16–18]. HMGB1 can be secreted by endothelial cells under certain conditions, secreted HMGB1 is found to play crucial roles in the regulation of endothelial cell functions like migration and angiogenesis. Moreover, extracellular HMGB1 was associated with impaired endothelium-dependent relaxation (EDR) by modulating TLR4/eNOS pathway [19]. However, the specific role and related working mechanism of HMGB1 in endothelial function are still not fully clear now. Thus, the aim of the present study was to examine the role of HMGB1 in terms of endothelial function and post ischemic recovery in endothelium-specific HMGB1 knockout mice (HMGB1ECKO).

☆ The work described in the article has not been previously presented in whole or partially.

* Corresponding author. Cardiovascular Department, The Second Xiangya Hospital of Central South University, middle Ren-Min road No.139, Changsha, Hunan, 410011, PR China.
E-mail address: zhuzhaowei@csu.edu.cn (Z. Zhu).

https://doi.org/10.1016/j.redox.2021.101890
Received 12 December 2020; Received in revised form 31 January 2021; Accepted 1 February 2021
Available online 5 February 2021

2. Materials and methods

2.1. Animals

All animal studies were reviewed and approved by the Central South University Institutional Animal Care and Use Committee and in compliance with the guidelines from Directive 2010/63/EU of the European Parliament on the protection of animals used for scientific purposes. HMGB1ECKO mice were prepared and bred in our laboratory by crossing floxed HMGB1 (HMGB1flox/flox) and VE-Cadherin promoter/enhancer (VE-CAD-Cre) mice. HMGB1 flox/flox mice and VE-CAD-Cre mice on C57BL/6 background were all purchased from Model Animal Research Center of Nanjing University (Nanjing, China). Transgenic mice used for experiments were confirmed by standard genotyping techniques. In parallel, HMGB1 levels in aorta, lung and extracts from the mouse lung endothelial cells were assayed by immunofluorescent staining and/or Western blot. Wild type mice used in this study were HMGB1flox/flox mice without the introduction of Cre recombinase. Mice were sacrificed by Carbon dioxide (CO2) inhalation with fixed time (3 min) and gradually increased concentration.

2.2. Blood pressure measurements

With a noninvasive computerized tail cuff system (CODA, Kent Scientific Corp, Torrington, Conn, USA), systolic, diastolic, and mean blood pressures were measured in conscious mice as described previously [20]. Three days measurements were performed after five days adaption of the environment. 20 measurements were obtained and averaged for each mouse on each day of blood pressure examination.

2.3. Vasomotor function

Vasomotor function of aortas was evaluated in vitro by isometric tension recording as described previously [21,22]. Briefly, aortas were removed from mice and placed immediately in oxygenated (95% O2, 5% CO2) Krebs' buffer (NaCl 118.3 mmol/L; KCl 4.7 mmol/L; CaCl2 2.5 mmol/L; MgSO4 1.2 mmol/L; KH2PO4 1.2 mmol/L; NaHCO3 25.0 mmol/L; glucose 11.1 mmol/L) at 4 °C. Each artery was cut into 3 mm segments with all adipose tissues removed. Then, each segment was suspended with tungsten wire (125 μm in diameter) in an organ chamber containing 15 ml oxygenated Krebs' buffer which was maintained at 37 °C. To measure the isometric tension, the ring was connected to a force transducer (Danish Myo Technology, Ann Arbor, MI. USA). All the tension data was recorded on a data acquisition system PowerLab (LabChart 7, AD Instruments, Sydney, Australia). After reaching a final optimal tension of 1 g in 30 min by gradually increased passive stretching, the segment was equilibrated for at least 30 min. The Krebs' solution was changed approximately every 30 min. To obtain a stable precontraction, the segment was challenged with 60 mM KCl lasted for 30 min. Then the KCl was washed out and the aortic segment rested for 30 min. Once the contraction plateau which was induced by phenylephrine (Phe; 10 μM; Sigma) reached, cumulative concentration-response curves were constructed to acetylcholine (ACh; 10-9 to 10-5 mol/L) or sodium nitroprusside (SNP; 10-9 to 10-5 mol/L; Sigma, St. Louis, MO, USA). NOS inhibitor Nω-nitro-L-arginine methyl ester (L-NAME, 0.3 mM, preincubated for 30 min) (Sigma, St. Louis, MO, USA) was used to verify NO-mediated relaxation during these tests. To determine the contribution of endothelium-derived ROS in ACh-induced relaxation, Polyethylene glycol-superoxide dismutase (PEG-SOD) (250 U/ml, pre-incubated for 45 min) was applied in the test to verify the inhibitory effect of this membrane permeable specific scavenger of ROS.

2.4. Organ culture of aortic segments

Mouse aortic segments (3 mm in length) were dissected in sterile PBS and infected with Ad-HMGB1 adenovirus or vector (108 pfu; Hanheng Biotechnology Co., Ltd., Shanghai, China) for 4 h in PBS. Further experiment was done in EGM-2 (Lonza, Walkersville, MD, USA) with 10% FBS.

2.5. Nitric oxide assay

Blood sample was obtained from mouse tail vein. Total NO in serum was tested with a colorimetric nonenzymatic nitric oxide assay kit (CalBiochem, San Diego, CA, USA) following the manufacturer's instructions.

2.6. Aortic ring assay

Aortic ring assays were carried out as described [23]. In brief, aortas were dissected and cut into 1-mm-thick rings. Individual rings were placed in basement membrane matrix which was growth factor-reduced (Matrigel; BD Biosciences, Franklin Lakes, NJ, USA). The aorta rings were incubated in medium (EGM-2; Lonza, Walkersville, MD, USA) containing 10% FBS for 4 days. At last, microphotographs of each well were taken and images were quantified (Image J, NIH, Bethesda, MD, USA) by measuring the number of sprouts originating from the rings.

2.7. Maintenance of endothelial cells and other cell lines

Human umbilical vein endothelial cells (HUVECs) were purchased from ATCC (Manassas, VA) and were maintained in EGM-2 (Lonza, Walkersville, MD, USA) with 10% FBS. Primary endothelial cells were isolated from lungs by immunoselection with CD31-antibody-coated magnetic beads. Sheep anti-rat-IgG Dyna beads were coated with monoclonal rat anti-CD31 antibody (BD Biosciences, Franklin Lakes, NJ, USA) according to the manufacturer's instructions. 6 to 8 day-old control and HMGB1ECKO pups were sacrificed, individual lung lobes were excised aseptically, without any bronchi and visible connective tissue. Then the harvest lungs were washed, finely minced and digested in 15 ml warm C/D solution (Roche Molecular Biochemicals, Indianapolis, IN, USA) for enzymatic digestion for 45 min at 37 °C on a rotator. The digested tissue was then filtered through a 100 μm cell strainer. After centrifuged at 1000 rpm for 10 min, the cell pellet was washed with EGM-2/10% FBS and centrifuged, resuspended in 1 ml EGM-2/10% FBS, which contained 1,000U/ml of heparin (Sigma, St. Louis, MO, USA), 50 ng/ml endothelial cell growth supplement (BD Biosciences, Franklin Lakes, NJ, USA), and penicillin-streptomycin. After incubation with 1 × 106 CD31-Ab-coated beads at room temperature for 12 min, bead-bound cells were separated from non-bead bound cells using a magnet. Bead-bound CD31 positive cells were resuspended in 2 ml EGM-2/10%FBS and plated out. After 6–7 and 11–13 days in culture, cells were reselected and purified twice. The cells labeling with Von Willebrand Factor (Abcam, Cambridge, MA, USA) and eNOS (Cell signaling, Danvers, MA, USA) were identified as endothelial cells.

2.8. Tube formation assay

Tube formation assay was performed as previously described. A 96-well, flat-bottom plate was prepared, coated with 50 μL Matrigel (BD Biosciences, Franklin Lakes, NJ, USA) per well. To promote gelling, the plate was kept at 37 °C for 1 h 2 × 104 cells in 100 μL EGM-2 medium (VEGF: 0.5 ng/ml) were seeded into each coated well and then incubated at 37 °C in a 5% CO2. The center of each well was photographed after 12 h using an inverted microscope (Nikon, Tokyo, Japan).

2.9. Cell proliferation assay

To test the viable cell number, HUVECs were plated in 96-well plates at a density of approximately 6000 cells/well in the medium 48 h after transfection with HMGB1 siRNA. After starved overnight (serum free), cells were treated with agents as indicated in each experiment. MTT

(Invitrogen, Carlsbad, CA, USA) assay kit was applied to determine the number of viable cells according to the manufacturer's instruction. MTT assay was repeated six times to ensure data reproducibility.

2.10. Cell hypoxia

In vitro HUVEC hypoxia model was used to mimic the hypoxia changes in vivo in this study. To induce hypoxia in vitro, confluent HUVECs were treated as described before [24]. In brief, confluent monolayers of HUVECs were placed into a hypoxia chamber (Thermo Fisher Scientific, Waltham, MA, USA). Chambers were closed and placed inside an incubator at 37 °C. 1% hypoxia was regulated by replacing ambient air in the chamber with a mixture of humidified nitrogen (95%) and CO2 (5%) until the 1% oxygen saturation was reached. The cells of various groups were kept in this hypoxic environment for 24 h.

2.11. Superoxide measurements

Dye dihydroethidium (DHE; Molecular Probes, Eugene, OR, USA) was applied for oxidative fluorescent, which was detected with confocal microscopy as described previously [22]. In brief, unfixed frozen aortic segments were stained with 10-6 mol/L DHE at 37 °C for 1 h in a dark humidified container. Then, DHE fluorescence was detected using a confocal microscope (Olympus, Tokyo, Japan) via a 590 nm long-pass filter.

Intracellular superoxide levels were detected in HUVECs with 5-(and-6)-chloromethyl-2′,7′-dichlorodihydrofluorescein diacetate, acetyl ester (CM-H2DCFDA), as described previously. Briefly, After 30 min incubation with CM-H2DCFDA (20 μM) at 37 °C, cells fluorescence was detected by a Synergy HT microplate reader (BIO-TEK) with excitation set at 490 nm and emission detected at 520 nm.

2.12. Enzyme-linked immunosorbent assay (ELISA)

Blood samples (0.5 ml) were collected by cardiac puncture under deep anesthesia. Serum was isolated from the blood after centrifugation at 3000 rpm for 20 min at 4 °C. HMGB1 concentrations were determined using the HMGB1 ELISA kit (IBL International GmbH, Hamburg, Germany).

2.13. siRNA transfection of HUVECs

HMGB1 siRNA (50 nM) (Santa Cruz Biotechnology, Santa Cruz, CA, USA) was added to 50–70% confluent HUVECs to deplete the HMGB1 followed the protocol provided by the manufacturer. Successful depletion of targeted protein was confirmed by Western blot analysis. All experiments were performed at 48 h post transfection.

2.14. Hind limb ischemia model

Hind limb ischemia animal model was performed as previously described [25]. In brief, all mice were anesthetized with isoflurane inhalation (3% induction and 1% maintenance; Webster Veterinary Supply, Inc., Sterling, MA, with 100% O2 as carrier). The proximal and distal portions of the femoral artery and the distal portion of the saphenous artery were ligated. The arteries and all side branches were dissected free and excised. The skin was carefully closed with 5-0 surgical sutures. Hind limb blood perfusion was determined with Laser Doppler Imaging (LDI) PeriScan PIM3 system (Perimed AB, Stockholm, Sweden) before and immediately after surgery and then at 7-day intervals, until the end of the study. The total follow-up was 28 days after surgery. Mice were placed on a heating plate at 40 °C during imaging, and excess hairs were removed from the limbs using depilatory cream. Results were expressed as the ratio between perfusion in the ischemic (right) and non-ischemic (left) hind limb to avoid the influence of ambient light and temperature.

2.15. Western blot analysis

Western blot analysis was performed by SDS/PAGE as described previously [19]. Tissues and cells were lysed with Cell LyticMT lysis buffer (Sigma) which contained a protease and phosphatase inhibitor mix (Roche Molecular Biochemicals, Indianapolis, IN, USA). The lysis process lasted for 20 min on ice. The protein content of the samples was determined by BCA assay (Pierce, Rockford, IL, USA) after centrifugation for 15 min at 12,000 g (4 °C). Equal amounts of protein (30 μg) were loaded onto SDS/PAGE and blotted onto nitrocellulose membranes (Whatman, Clifton, NJ, USA). Immunobloting was performed with antibodies directed against each target molecule: Akt (1:1000; Cell signaling, Danvers, MA, USA); phosphorylated- Akt ser473 (1:500; Cell signaling, Danvers, MA, USA); eNOS (1:1000; Cell signaling, Danvers, MA, USA), phosphorylated-eNOS ser1177 (1:500; Cell signaling, Danvers, MA, USA), HMGB1 (1:1000; Abcam, Cambridge, MA, USA), VEGF (1:1000, Abcam, Cambridge, MA, USA), β-actin (1:10000; Cell signaling, Danvers, MA, USA), GAPDH (1:1000, Cell signaling, Danvers, MA, USA), α-Tubulin (1:1000; Cell signaling, Danvers, MA, USA). Proteins were detected by ECL chemiluminescence after incubation with HRP-conjugated secondary antibody (Santa Cruz Biotechnology, Santa Cruz, CA, USA). NIH Image J software was used to quantify the bands.

2.16. Immunofluorescence and immunohistochemistry analysis

Harvested from mice, aortas and lungs were perfused with PBS and then with 4% paraformaldehyde for 2 h. After dehydration with sucrose gradient, tissues were embedded in OCT and then cut into sections with 6 μm thickness. The sections were then blocked with 3% normal goat serum. Consequently, tissues were incubated overnight at 4 °C with primary antibodies (HMGB1, CD31, F4/80, Abcam, Cambridge, MA, USA) diluted with 2% bovine serum albumin in PBS. Tissues were incubated with specific secondary antibodies for 1 h at 37 °C after three washes with PBS. At last, tissues were stained with DAPI to visualize cell nuclei and mounted in gelvatol for fluorescent imaging. A confocal microscope (Olympus Fluoview 500, Japan) was used for immunofluorescence staining images.

Tissues were also fixed in 4% paraformaldehyde and then embedded in paraffin for other tests. Tissues with thickness of 5 μm were deparaffinized and processed for hematoxylin and eosin (H&E) staining or incubated with a HMGB1 antibody (Abcam, Cambridge, MA, USA). To avoid the primary antibodies, negative controls were used. A digital camera (Nikon, Japan) was used to capture five randomly selected fields from each sample and to count visible capillaries (positive for HMGB1).

2.17. Adenovirus transduction of murine skeletal muscle

After anesthetized, adenovirus vectors expressing HMGB1 or SOD2 or control virus was injected in 3 different sites of the left adductor muscle (1 × 1011 viral genomes/limb) of 8-week-old mice. Hind limb ischemia was induced 3 days after virus injections. Laser Doppler was applied to test limb perfusion on day 0, 1, 7, 14, 21 and 28 post ischemia. Western blotting analysis was used for HMGB1 and SOD2 expression.

2.18. Statistical analysis

For ex-vivo and in vitro experiments, data were obtained from at least 3 independent experiments. For in vivo experiments, data were obtained from at least six mice/per group. The data are presented as mean ± SD. Differences between two groups were evaluated with unpaired Student's t-test or a Mann-Whitney nonparametric test after the variables were ranked. For three or more groups, data were compared by one-way ANOVA followed by Tukey post-hoc analysis. Comparisons including two factors were performed by two-way ANOVA. All statistical analysis involved was applied with GraphPad Prism 8.0 (GraphPad Software Inc, San Diego, CA, USA). A P value of <0.05 was considered

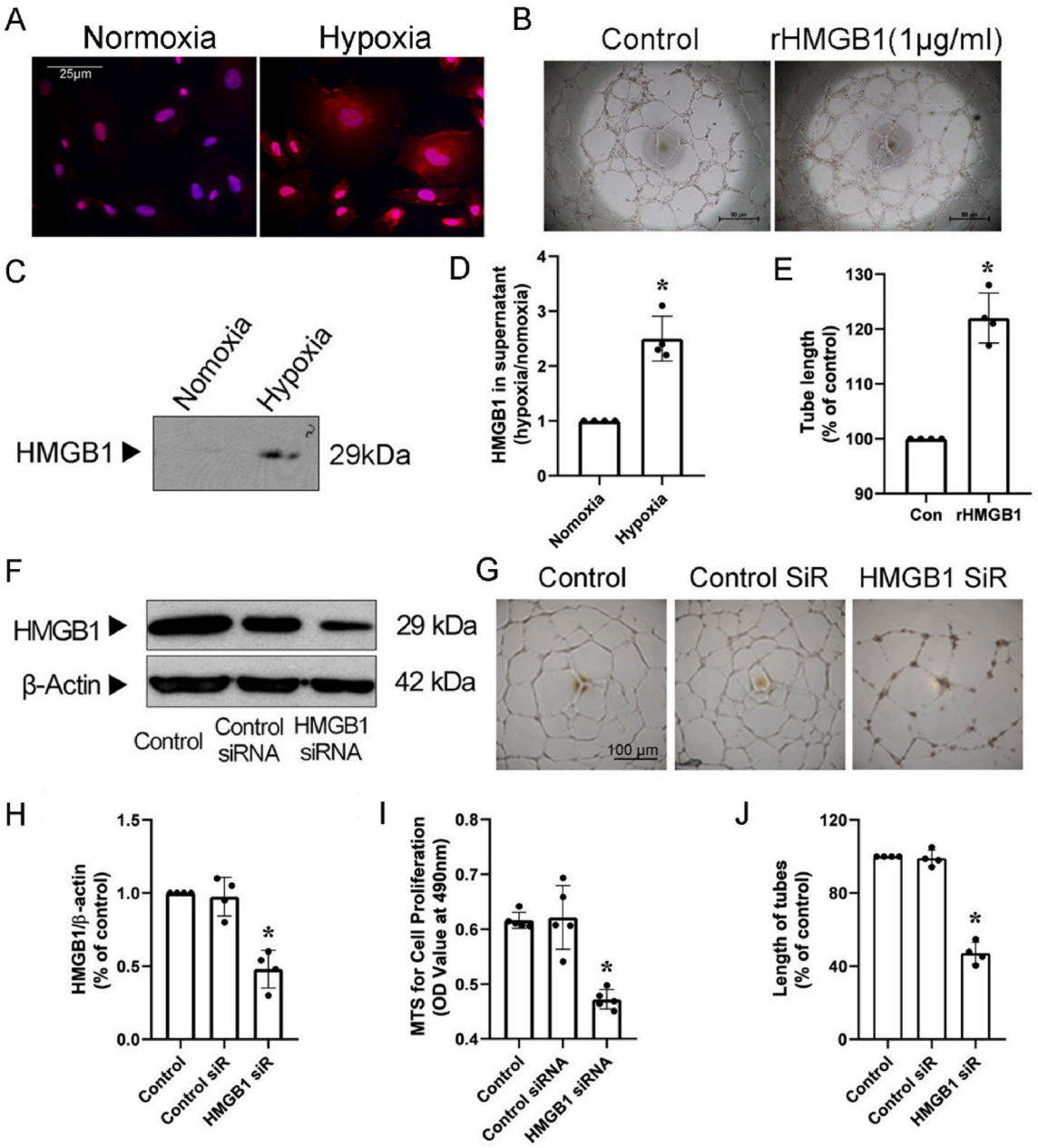

Fig. 1. HMGB1 mediates important roles in HUVECs. A, Immunofluorescent staining (HMGB1, red; DAPI, blue; scale bars, 25 μm) for HUVECs exposed to hypoxia (1%) for 24 h. Photomicrographs are representative of three independent experiments. B, Representative capillary-like networks (tube formation, scale bars, 50 μm) of HUVECs with or without purified recombinant human HMGB1 treatment. C and D, Representative Western blot (C) and quantitative analysis (D) of HMGB1 in the cell media of HUVECs exposed to hypoxia. E, Total tube length from each of four randomly chosen fields was quantified using the image analysis software image. F and H, HMGB1 silencing of HUVECs. F, representative blots for HMGB1 silencing of HUVECs. H, HMGB1 siRNA silenced 60% of HUVEC HMGB1 protein expression. G, J, I, Tube formation and proliferation were tested after HMGB1 siRNA transfection. G, Representative capillary-like networks of HUVECs after HMGB1 silencing. (scale bars, 100 μm). and J, Quantifications of EC network formation in HUVECs with HMGB1 siRNA. I, the proliferation of HUVECs transfected with HMGB1 siRNA was decreased by 24%. Data are the average of triplicates from single experiments that were independently repeated 4–5 times. Band densities were normalized with that of β-actin. Comparisons were performed by using two-tailed unpaired Student's t-tests for D, E. Comparisons were performed by using one way ANOVA for H, I, J. (*$P < 0.05$). (For interpretation of the references to color in this figure legend, the reader is referred to the Web version of this article.)

significant.

3. Results

3.1. HMGB1 mediates important roles in endothelial cells

HMGB1 translocation was assessed in HUVECs under hypoxia conditions. After 24 h hypoxia, HMGB1 expression increased in HUVECs (Supplementary Fig. 1), and the HMGB1 expression in cytoplasm of HUVECs was higher post hypoxia as compared to normoxia conditions, which indicated that HMGB1 translocated from nuclear to cytosol after hypoxia (Fig. 1A). In addition, after translocated to cytosol, HMGB1 was further released to supernatant. This finding was confirmed by WB where supernatant HMGB1 levels were significantly higher post hypoxia (Fig. 1C and D). Next, to identify the role of extracellular HMGB1 in endothelial cells, we stimulated HUVECs with recombined HMGB1 protein, and in agreement with published results, tube formation increased by about 26% compared with control (Fig. 1B, E). Then, we

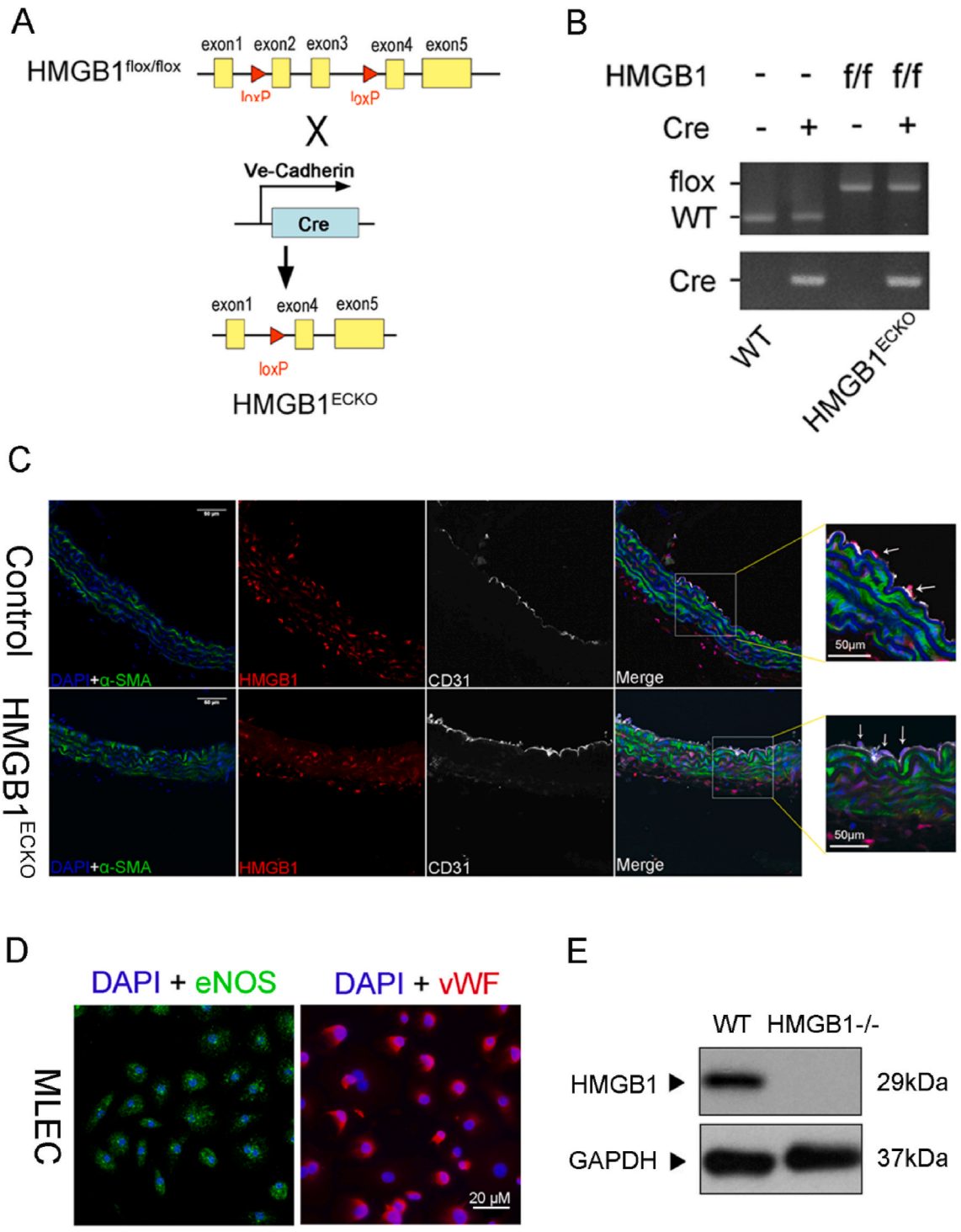

Fig. 2. Generation and characterization of HMGB1ECKO mice. A, Schematic diagram of the transgenic mice used to generate HMGB1ECKO mice. B, PCR analysis for HMGB1ECKO mice genotype. C, IF stain of HMGB1 (red) and CD31 (white) in aortas from HMGB1ECKO and control mice. Scale bar = 50 μm. D. Characterization of MLECs. Subconfluent MLECs (third passage) grown on glass cover slips were stained with endothelial surface markers, vWF, using anti-vWF antibody (primary) and a FITC-labeled secondary antibody. eNOS antibody (primary) and a Cys 3 secondary antibody. Scale bar = 20 μm. E. Representative Western Blot of HMGB1 expression in MLEC from control and HMGB1ECKO mice. Data are the average of triplicates from single experiments that were independently repeated 3 times. (For interpretation of the references to color in this figure legend, the reader is referred to the Web version of this article.)

explored the function of intracellular HMGB1 in endothelial cells by silencing HMGB1 expression with siRNAs. After 48 h transfection, total HMGB1 levels were reduced by 60% post HMGB1 siRNA treatment compared with scramble control RNAs (Fig. 1F, H). Proliferation results showed that HMGB1 silencing reduced the number of cells by 48% (Fig. 1I) compared with controls. Silencing of HMGB1 also inhibited sprouting by 52% as assessed by in vitro tube formation assay (Fig. 1G and J). These results suggest that both extra- and intracellular HMGB1 play an important role in endothelial cells in vitro.

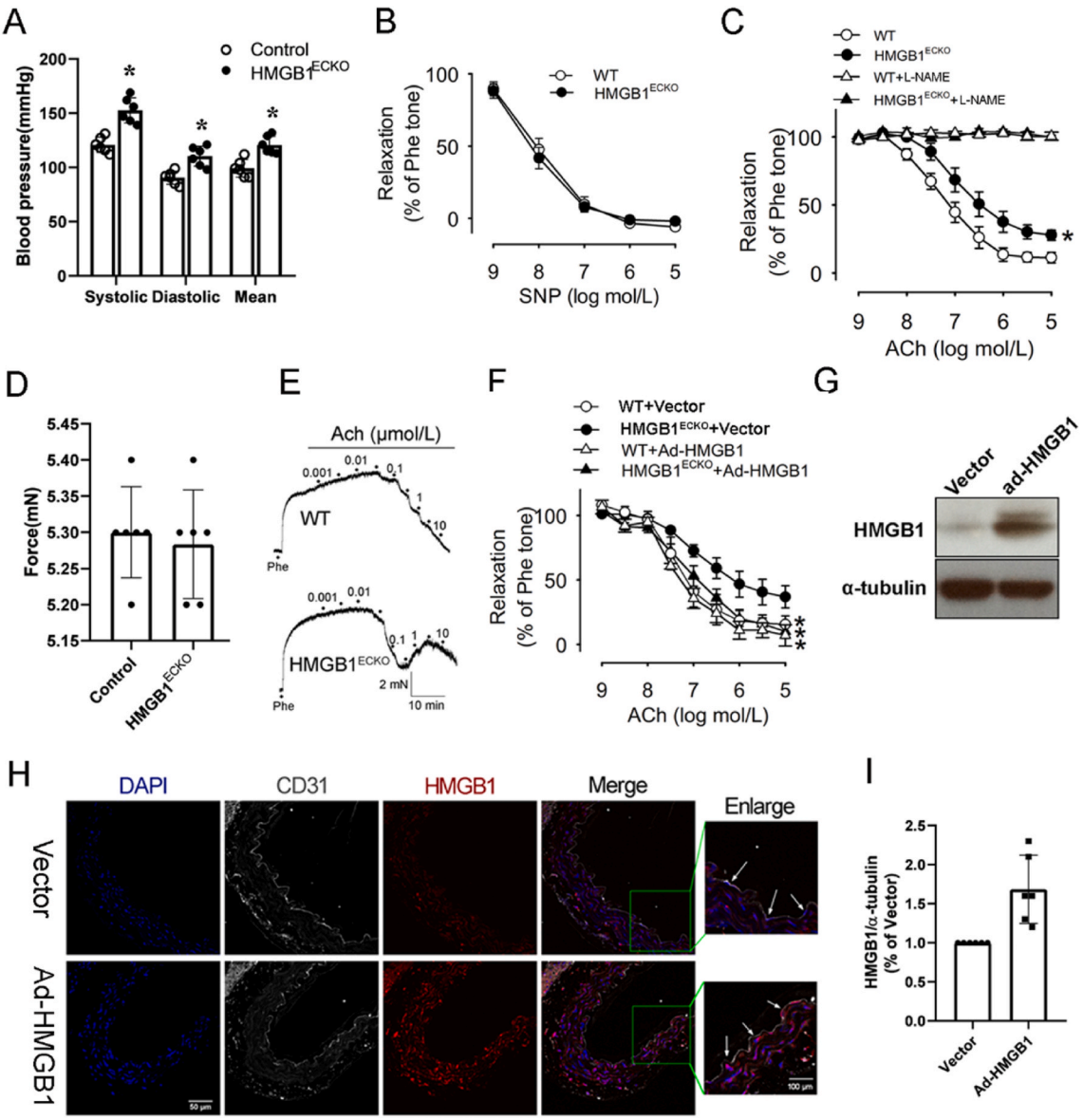

Fig. 3. Impaired EDR in HMGB1ECKO mice. A, Blood pressure including systolic, mean, and diastolic blood pressures from male control and HMGB1ECKO mice at three months was measured using the noninvasive computerized tail cuff system (n = 10). *P < 0.05 vs. control. B, Response to sodium nitroprusside in mice aortas. Vessels were precontracted with phenylephrine. All values are mean ± SD. C, Relaxation response to acetylcholine of aortas obtained from control and HMGB1ECKO mice with or without L-NAME. D, response to phenylephrine of aortas from control and HMGB1ECKO mice. E, representative response curve of aortas from control and HMGB1ECKO mice. F, Relaxation response to acetylcholine of aortas from HMGB1ECKO mice with ad-HMGB1 transfection or ad-Vector transfection. G, I, Representative Western Blot and quantitative analysis of HMGB1 expression in aortas from ad-HMGB1 or ad-Vector group. H, IF stain of HMGB1 in aortas transfected with or without ad-HMGB1 from HMGB1ECKO mice. (HMGB1, red; DAPI, blue; CD31, white; scale bars, 50 μm, 100 μm for enlarged window). Data are the average of triplicates from single experiments that were independently repeated 3 times. Comparisons were performed by using two-way ANOVA. (*$P < 0.05$). (For interpretation of the references to color in this figure legend, the reader is referred to the Web version of this article.)

3.2. Generation and analysis of HMGB1ECKO mice

To verify the biological role of HMGB1 in vascular endothelial cells in vivo, HMGB1flox/flox mice were crossbred with VE-CAD-Cre mice to generate VE-CAD-Cre/HMGB1flox/flox mice (referred as HMGB1ECKO) (Fig. 2A). The littermate HMGB1flox/flox/Cre−/− mice were used as controls. Grossly, there was no apparent phenotypic differences or abnormalities of HMGB1ECKO mice which were born healthy and fertile.

To confirm endothelium-specific HMGB1 deletion in HMGB1ECKO mice, genotyping was performed in HMGB1ECKO mice and control littermates (Fig. 2B) with PCR. Next, we performed double-immunofluorescence labeling for HMGB1 and CD31 in aortas from control mice and HMGB1ECKO mice. HMGB1 expression was found colocalized with CD31 in the endothelium of aortas from control mice, while HMGB1 expression was absent in the endothelium of aortas from HMGB1ECKO mice (Fig. 2C). Obviously, HMGB1 expression can be found in smooth muscle cells with α-SMA stain in aorta walls from both group of mice (Fig. 2C). Immunohistochemistry stain of HMGB1 in aortas was also consistent with this result (Supplementary data Fig. 2). To confirm the efficiency of HMGB1 knockdown in endothelial cells, mouse primary lung endothelial cells (MLECs) were also isolated and then stained with vWF and eNOS (Fig. 2D). As expected, HMGB1 was barely detectable in MLECs from HMGB1ECKO mice (Fig. 2E), confirming the effective HMGB1 deletion in HMGB1ECKO mice.

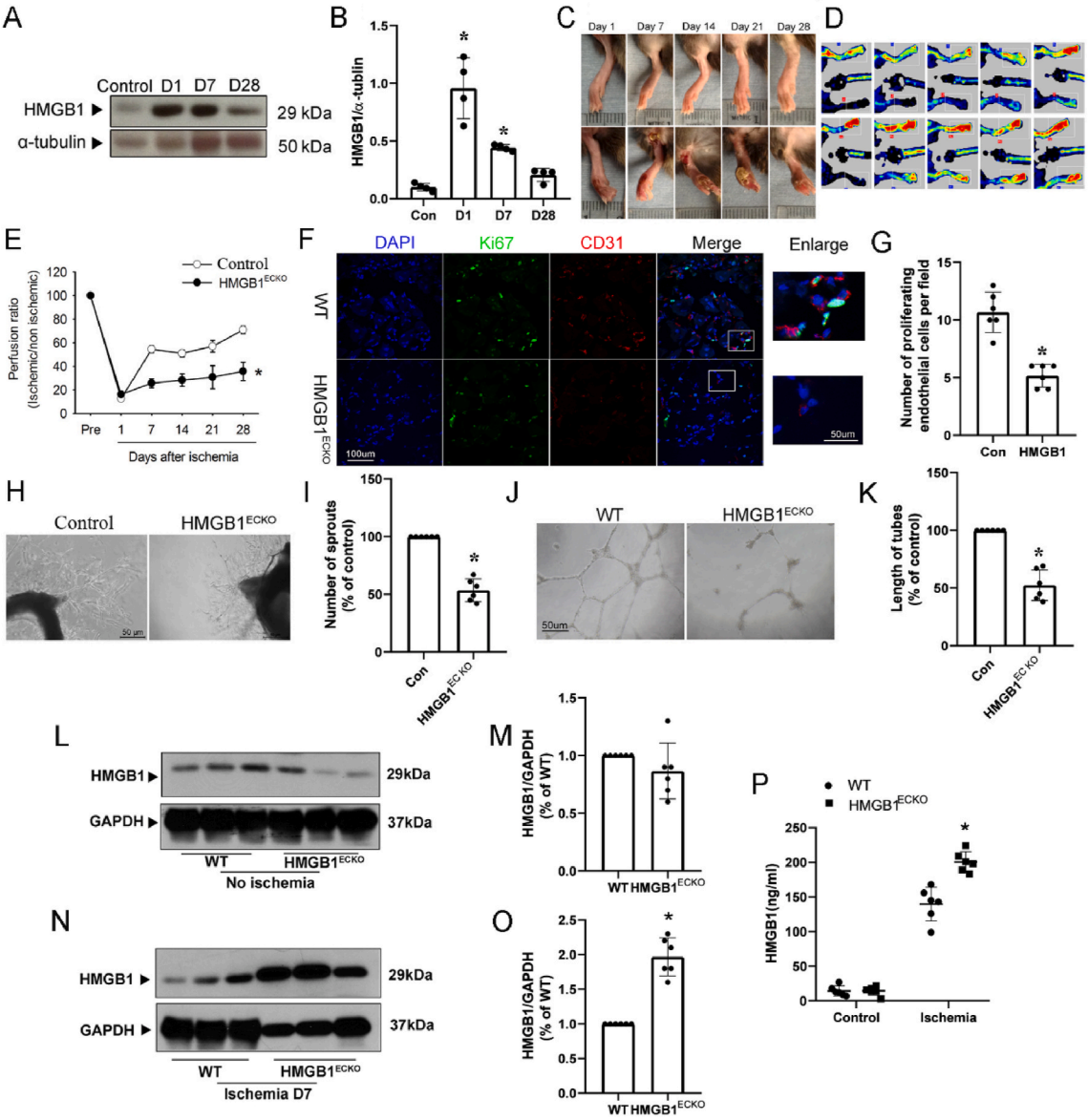

Fig. 4. Ischemia-initiated blood flow recovery and angiogenesis were impaired in HMGB1ECKO mice. A, Representative Western Blot of HMGB1 expression in ischemic muscles on day 0, 1, 7 and 28. B, Quantitative densitometry analysis of HMGB1 expression in ischemic muscle on day 1 and 7 and 28. C, HMGB1ECKO mice developed necrotic toes at 7 days–14 days after femoral artery resection while WT littermate mice did not. Representative images for necrotic toes after surgery were shown. D, Representative images of Laser Doppler blood flow on day 0, 1, 7, 14, 21 and 28 post ischemia. E, Blood flow in ischemic hind limb was measured. Results were expressed as a ratio of the right (ischemic) to left (control, nonischemic) limb perfusion. F. Proliferated endothelial cells were marked with IF stain of CD31 and ki67. DAPI, blue; CD31, red; ki67, green; scale bars, 100 μm. G. Quantification of capillary density, calculated as the number of endothelial cells positive with both CD31 and Ki67 per field. H and I, Microvessel sprouting in aortic ring assay. Representative micrographs and statistic results of sprouting microvessels from aortic ring grown in the EGM-2 medium after 4 days were shown. vs control. J and K, Tube formation of MLEC from WT and HMGB1ECKO mice. L, M, Representative Western Blot and quantitative analysis of HMGB1 expression in non-ischemic muscles from WT and HMGB1ECKO. N, O, Representative Western Blot and quantitative analysis of HMGB1 expression in ischemic muscles from WT and HMGB1ECKO. P, Serum HMGB1 levels in WT and HMGB1ECKO before and after HLI procedure. Data are the average of triplicates from single experiments that were independently repeated 3 times. Comparisons were performed by using two-tailed unpaired Student's t-tests for G, I, K, M, O, P, one way ANOVA for B and two-way ANOVA for E. (n = 6. *$P < 0.05$, compared with WT or Control). (For interpretation of the references to color in this figure legend, the reader is referred to the Web version of this article.)

3.3. Loss of endothelial HMGB1 triggers impairment of EDR

As endothelial cells are crucial in regulating blood pressure, we measured blood pressure on HMGB1ECKO mice. As shown in Fig. 3A, both diastolic blood pressure (98 ± 11 mm Hg versus 86 ± 8 mm Hg, $P < 0.05$) and systolic blood pressure (148 ± 8 mm Hg versus 117 ± 9 mm Hg, $P < 0.05$) were significantly increased in HMGB1ECKO mice than in control littermates. Besides, mean blood pressure (mBP) was also significantly higher in HMGB1ECKO mice (125 ± 8 mm Hg) than in control mice (94 ± 8 mm Hg, $P < 0.05$). Above results demonstrated that loss of HMGB1 in the endothelium resulted in higher blood pressure.

Vasomotor function is an important peripheral component for the blood pressure regulation. As the blood pressure increased significantly in HMGB1ECKO mice, we investigated the effect of endothelial HMGB1 deletion on vasomotor function. As shown in Fig. 3D, phenylephrine (PE) (10-6 M)-induced contraction force was similar between the aortas from control (6.46 ± 0.71 mN) and HMGB1ECKO mice (6.28 ± 1.26 mN, $P > 0.05$). Increasing doses of acetylcholine (ACh; 10-10 to 10-4 M) were

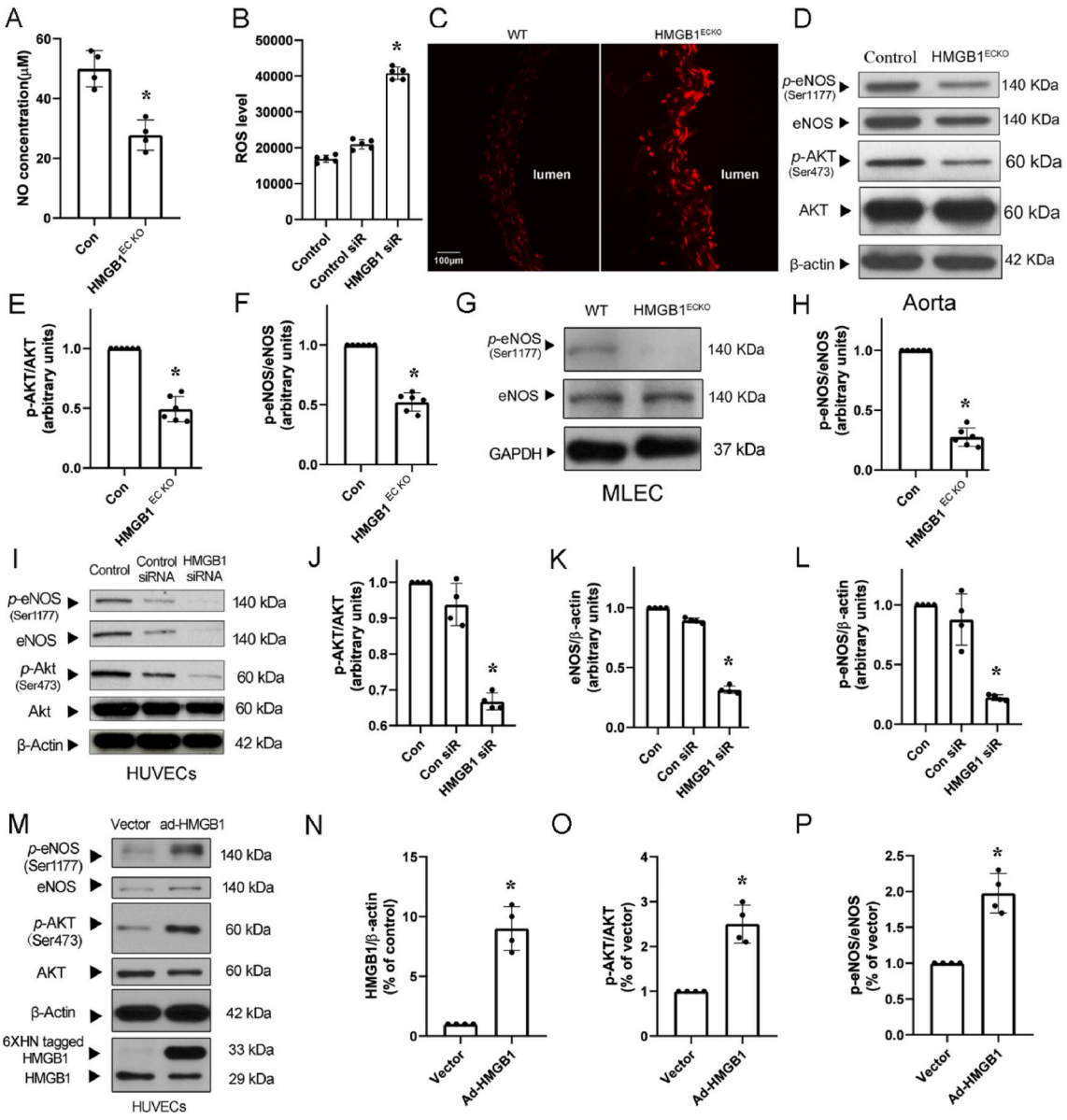

Fig. 5. NO decreased and ROS increased after loss of HMGB1. A, NO was measured in serum from WT and HMGB1ECKO mice. B, ROS production in HUVECs after HMGB1 siRNA transfection. C, DHE staining of aortas from WT and HMGB1ECKO mice. D, Representative Western Blot of p-eNOS, eNOS, p-AKT and AKT in aortas from WT and HMGB1ECKO mice. E and F, Quantitative densitometry analysis showed p-AKT/AKT and p-eNOS/eNOS ratio were decreased significantly in aortas from HMGB1ECKO mice. G and H, Representative Western Blot of p-eNOS and NOS in MLEC. p-eNOS level was decreased in MLEC from HMGB1ECKO mice. I, Representative Western Blot of p-eNOS, eNOS, p-AKT and AKT in HUVECs transfected with HMGB1 siRNA. J, K and L, Quantitative densitometry analysis showed p-AKT/AKT and p-eNOS/eNOS expression were decreased significantly. M, Representative Western Blot of HMGB1, p-eNOS, eNOS, p-AKT and AKT in HUVECs after transfected with ad-HMGB1. N, O and P, Quantitative densitometry analysis showed HMGB1 expression increased in HUVECs after ad-HMGB1 transfection. p-AKT/AKT and p-eNOS/eNOS ratio were rescued significantly. Band densities were normalized with that of β-actin or GAPDH. Comparisons were performed by using two-tailed unpaired Student's t-tests for A, E, F, H, N, O, P and one-way ANOVA for B, J, L. (n = 4–6; $^*P < 0.05$).

added after contractions plateau was reached and concentration-dependent relaxations were tested in aortas of mice. As shown in Fig. 3C and E, ACh-induced relaxations were significantly impaired in aortas derived from HMGB1ECKO mice (Fig. 3C and E). However, after pretreated with an eNOS inhibitor (L-NAME, 10-4 M) for 30 min, increased dose of ACh induced similar responses in the aortas of two strains (Fig. 3C). Above results showed that the impaired relaxations in the HMGB1ECKO aorta was mediated by eNOS pathway. Consistently, there was no difference of relaxations caused by endothelium-independent agent sodium nitroprusside (SNP) between control and HMGB1ECKO mice (Fig. 3B), indicating that HMGB1 deficiency only impairs endothelial function in HMGB1ECKO mice. Overall, these results demonstrate that endothelial deletion of HMGB1 impairs EDR.

To confirm the role of HMGB1 in vasomotor function, we overexpressed HMGB1 in aortas from HMGB1ECKO mice after incubation with ad-HMGB1 virus (Fig. 3G, H, 3I) and then the vessel function was tested. As expected, the ACh-induced relaxations were partly rescued post HMGB1 overexpression in HMGB1ECKO mice (Fig. 3F).

3.4. Endothelial HMGB1 mediates ischemia-initiated blood flow recovery and angiogenesis

To investigate the role of HMGB1 in postnatal angiogenesis, we first examined HMGB1 expression in ischemic hind limb induced by surgical arteriectomy of the right femoral artery. Lower limbs of the ischemic (right) and nonischemic (left) legs were harvested on days 1, 7, 14 and

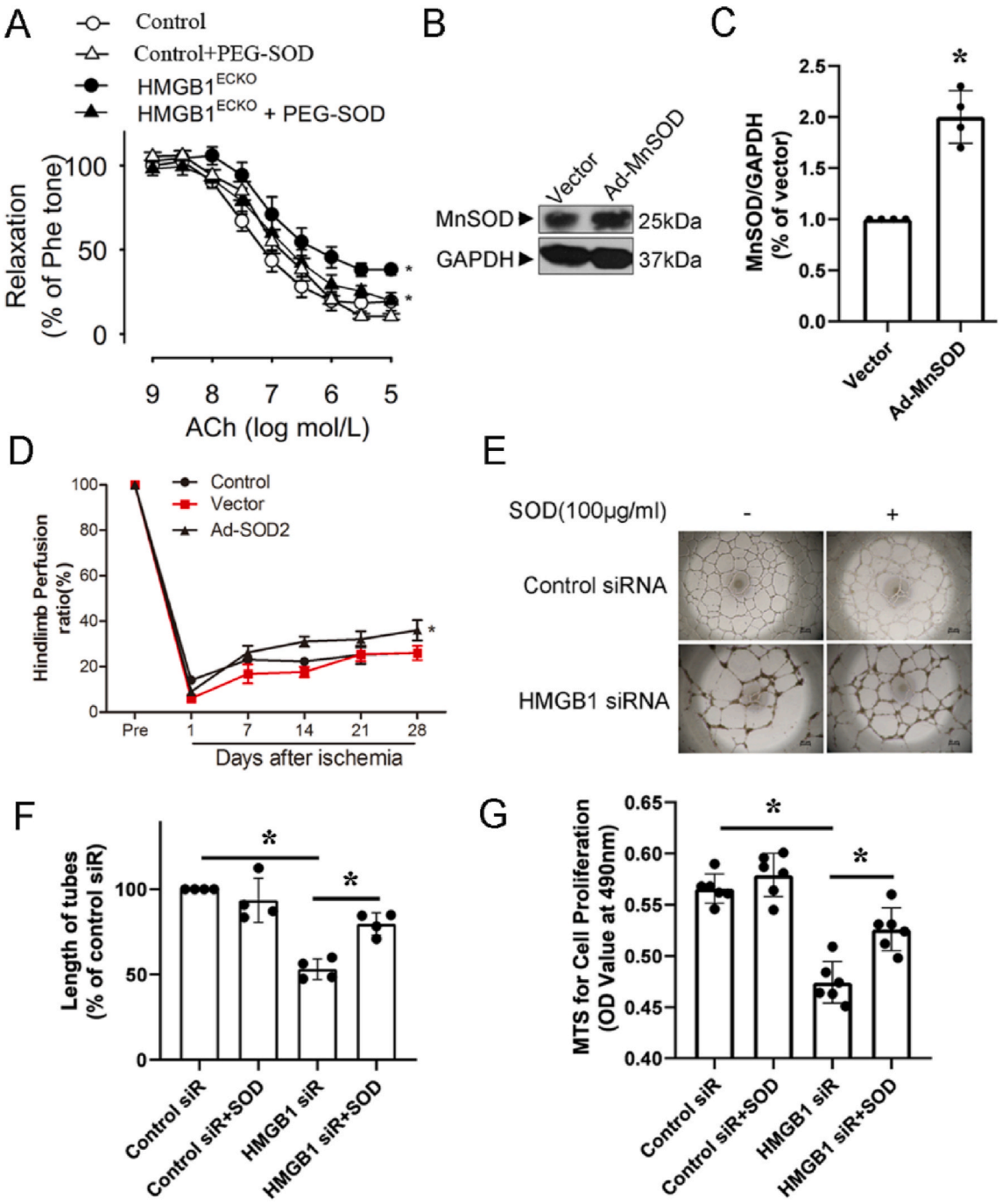

Fig. 6. SOD rescued endothelial dependent EDR and angiogenesis. A, EDR was tested in aortas from HMGB1ECKO mice with or without pre-incubation of PEG-SOD. B, HMGB1ECKO mice were injected with Ad-GFP or Ad-SOD2 and SOD2 levels examined in the adductor muscle group by Western Blot after 4 days of infection (C). Ad-SOD2 improved the time course of blood flow recovery (D). HUVECs transfected with HMGB1 siRNA were treated with or without PEG-SOD (100 μg/ml), then proliferation(G) and tube formation were tested. (E, F) Representative images were shown. Comparisons were performed by using two-tailed unpaired Student's t-tests for C, one-way ANOVA for F, G and two-way ANOVA for A, D. (n = 4–6, $^*P < 0.05$).

28 after surgery, and the protein expression of HMGB1 was determined by Western blotting with anti-HMGB1 antibody. Generally, HMGB1 expression was significantly upregulated in the ischemic lower hind limb. In detail, HMGB1 expression increased at day 1 and day 7 and declined to the basal level at day 28 post operation (Fig. 4A and B) in WT mice. Similar HMGB1 expression change was found in HMGB1ECKO mice (Supplementary Fig. 3). These results indicate HMGB1 might play a potential role in ischemia and angiogenesis.

Next, to precisely verify functional defects in HMGB1ECKO mice, laser speckle blood flow imager was applied to measure the ischemic and nonischemic limb perfusion before surgery and then at day 1, 7, 14 and 28 post surgery. As shown in Fig. 4C, D, E, blood flow recovered gradually and returned to almost normal levels on day 28 post operation in control group. However, the recovery of blood flow in ischemic hind limbs of HMGB1ECKO mice was poor throughout the whole post-operative period compared with that in control mice. Accordingly, control mice showed limited necrosis of toes, while hind-limb autoamputations occurred in 20% of HMGB1ECKO mice on day 28 after ischemic surgery, suggesting retarded blood flow recovery in HMGB1ECKO mice post ischemic insult (Fig. 4C and D).

Capillary vessels identified by CD31 and ki67 staining were markedly increased in ischemic muscle of control mice 4 weeks after surgery. While CD31 and ki67 staining positive cells in ischemic muscle from HMGB1ECKO mice were significantly lower compared with that in control mice (Fig. 4F and G).

To further investigate the role of HMGB1 in angiogenesis, we performed ex vivo angiogenesis assay of the aorta ring and capillary-like tube formation of endothelial cells derived from HMGB1ECKO mice or control mice. In the aorta ring assay, the number of sprouting microvessels from HMGB1ECKO mice in the presence of VEGF was dramatically reduced as compared to control mice (Fig. 4H and I). In the tube formation assay, mouse lung endothelial cells isolated from HMGB1ECKO mice and control mice were used. As shown in Fig. 4J and K, the capillary-like tube formation in the presence of VEGF was significantly enhanced in control endothelial cells, while capillary-like tube formation was significantly impaired in HMGB1 deficient endothelial cells compared with that in control endothelial cells.

To test the effect of EC-deficiency of HMGB1 on the upregulation of HMGB1 induced by HLI procedure, we evaluated the protein expression in muscle tissue and the serum in both HMGB1ECKO mice and WT controls. Based on the previous results, HMGB1 expression in ischemic tissues increased in day 1 and day 7 post operation, but there is a smaller heterogeneity in day 7. So we measured the HMGB1 levels on day 7 post ischemia. Compared with control mice, HMGB1 expression in non-ischemic muscle from HMGB1ECKO mice showed mild decrease without statistical significance pre-operation (Fig. 4L, M, and Supplementary Fig. 4). Serum level of HMGB1 was similar in both groups pre-operation (Fig. 4P). HMGB1 expression was significantly higher in ischemic muscle from HMGB1ECKO mice in day 7 post operation, compared with that from control mice (Fig. 4N, O, and Supplementary Fig. 4). Similar trend was found in the serum level of HMGB1 measured by ELISA in the two groups (Fig. 4P). Consistent with above results, local inflammation evaluated with macrophage cell maker F4/80 showed that there were more macrophage cells accumulated in ischemic muscle compared with that in non-ischemic muscle, especially in HMGB1ECKO mice (Supplementary Fig. 4), and VEGF expression in ischemic muscle from HMGB1ECKO mice was also higher compared with that in ischemic muscle from WT mice (Supplementary Fig. 5).

3.5. Loss of endothelial HMGB1 decreased NO and increased ROS

To identify potential role and mechanisms underlying the HMGB1 deficiency mediated dysfunction of endothelial cells, we first detected the NO level in serum from control and HMGB1ECKO mice at base conditions. Consistently, serum NO level was significantly reduced in HMGB1ECKO mice than that in control mice (Fig. 5A).

We next evaluated the effects of HMGB1 deletion on ROS production in aortas from control and HMGB1ECKO mice with DHE stain. The ROS level was significantly increased in aortas from HMGB1ECKO mice (Fig. 5C). In line with this finding, ROS level was also increased in HUVECs post HMGB1 siRNA transfection (Fig. 5B).

As eNOS is the only enzyme which can produce NO in endothelial cells. We next measured eNOS activity in aorta tissue from control and HMGB1ECKO mice via Western blot analysis. The protein levels of phosphorylated eNOS at Ser1177 (p-eNOS) and total eNOS in aorta tissues were significantly lower in HMGB1ECKO mice than in control mice (Fig. 5D, F). Because Akt is a well-characterized regulator of eNOS activity, we monitored the activated form of Akt: phosphorylation of Akt. p-Akt/Akt ratio was significantly decreased in aorta tissues in HMGB1ECKO mice as compared to control mice (Fig. 5E), indicating HMGB1 regulated eNOS activity through Akt pathway. To confirm this finding, we tested eNOS phosphorylation in primary lung endothelial cells from the two groups, the p-eNOS/eNOS ratio was significantly lower in HMGB1ECKO mice than in control mice (Fig. 5G and H). Besides, 48 h after transfection, eNOS phosphorylation at Ser1177 was significantly lower in HUVECs transfected with HMGB1 siRNA as compared with control siRNA (Fig. 5I, J, K, L). While overexpression of HMGB1 in HUVECs with ad-HMGB1 virus significantly upregulated p-eNOS/eNOS and p-Akt/Akt ratio (Fig. 5M, N, O, P). These results collectively suggest that HMGB1 may regulate eNOS activation through Akt pathway.

3.6. SOD rescued endothelial function dependent EDR and limb ischemia in HMGB1ECKO mice

As ROS level increased in response to HMGB1 deficiency, which might subsequently reduce NO activity and endothelial cell dysfunction. To test this hypothesis, we observed if anti-ROS treatment with SOD could recover functions of endothelial cells with HMGB1 deficiency. The aortas derived from HMGB1ECKO mice were incubated with PEG-SOD before adding phe. As expected, EDR were rescued partly in aortas from HMGB1ECKO mice post PEG-SOD treatment (Fig. 6A).

To test whether local gene delivery of SOD could rescue the critical limb ischemia in HMGB1ECKO mice, a constitutively active form of SOD2 was applied to this model by Ad-SOD2 virus. The delivery method and activity of this construct has been well characterized [26]. As shown in Fig. 6B, intramuscular injection of Ad-SOD2 into the ischemic adductor muscle resulted in increased expression of SOD2 (detected at 4 days after infection) as compared with control virus injection (Fig. 6C). Administration of Ad-SOD2, but not Ad-Vector into the ischemic adductor muscle at the time of ischemia induction markedly improved blood flow perfusion at 2 and 4 weeks post ischemia (Fig. 6D).

In addition, we also treated HUVECs with PEG-SOD after transfection with HMGB1 siRNA. Consistently, PEG-SOD (100 μg/ml) rescued proliferation and tube formation of HUVECs transfected with HMGB1 siRNA (Fig. 6E, F, G).

4. Discussion

This study was designed to clarify the cell specific roles of HMGB1 in endothelial cells function. Results showed that endothelium-specific HMGB1 deletion decreased NO production and impaired endothelial function, resulting in hypertension and retarded blood flow recovery post ischemic hind limb injury in mice. Above results indicate that HMGB1 is essential to maintain normal endothelial function through regulating the production of NO via Akt pathway and ROS production. To our best knowledge, this is the first report describing the role of HMGB1 in HMGB1ECKO mice model.

Previously, the consequences of HMGB1 deficiency were difficult to define since mice deficient in HMGB1 died shortly after birth [3]. Therefore, conditional HMGB1 knockout mice (HMGB1 endothelial cell specific knockout) were developed. There are mainly two ways to knock out genes specially in endothelial cells. One is Tie1/Tie2-Cre system, the other is vascular endothelial cadherin (VE-cadherin, also known as Cdh5) -Cre system. While Tie1/Tie2-Cre is broadly expressed in hematopoietic lineages, neuronal populations, and the mesoderm [27,28], VE-CAD-Cre is more specifically expressed in endothelial cells [29]. Therefore, VE-CAD-Cre system was applied to generate EC specific knock out mice in this study to explore the functions of HMGB1 in endothelial cells.

Previous researches indicated that HMGB1 could promote angiogenesis in cancer growth and ischemic disease [3,23,25,30]. It is well known that extracellular HMGB1, as a DAMP, could induce angiogenic effect through TLR4 or RAGE pathway and the downstream effector VEGF/VEGFR2. In our study, HMGB1 level in ischemic tissue and peripheral circulating was higher in HMGB1ECKO mice as compared to that in WT mice (Fig. 4), however, the ischemic recovery capacity was less in HMGB1ECKO mice as compared to that in WT mice (Fig. 4), indicating higher HMGB1 is not linked with promoted angiogenesis in HMGB1ECKO mice. Based on above results, we speculated that extracellular HMGB1 might play a minor role on promoting angiogenesis in the absence of intact EC HMGB1. More importantly, intracellular

HMGB1 of endothelial cells preserves endothelium function and might be a prerequisite for post ischemic angiogenesis. Future studies are warranted to provide direct evidence to show the exact role of intracellular HMGB1 on promoting the angiogenesis in these models.

Previous studies showed that intracellular HMGB1 could stabilize cell functions, which would support above speculation. It was shown that hepatocyte specific HMGB1 knockout resulted in increased DNA damage and nuclear instability of hepatocyte, which aggravated liver ischemia-reperfusion injury [5]. Pancreas-specific HMGB1 knockout disrupted the cell stability and induced more severe impairment during acute pancreatitis in mice [6]. Intracellular HMGB1 also contributed to the protection of mice from bacterial infection post knock down HMGB1 in either macrophages or intestinal epithelial cells [7,8]. Although DNA damage and nuclear instability were not tested in this study, endothelial deletion of HMGB1 caused endothelial dysfunction with decreased NO production and increased ROS level.

Loss of HMGB1 in cells will cause severe inflammatory responses after stress in animals [5,6]. In fact, more macrophages infiltrated in the ischemic areas in HMGB1ECKO mice than in WT mice, which can also explain higher HMGB1 expression in ischemic muscles of HMGB1ECKO mice. Besides, serum HMGB1 was also higher in HMGB1ECKO mice than in WT mice in this study, which is consistent with the increased inflammation level. The retarded ischemia recovery of HMGB1ECKO mice might further increase the number of macrophages and necrotic cells, which might be the source of consequently elevated serum HMGB1. Although HMGB1 can be released from several cell types including endothelial cells, macrophages and necrotic cells during ischemic process, it is difficult to know if there are different roles of released HMGB1 from different cell types. Previous studies demonstrated that the role of HMGB1 varied based on its different redox state [3,31]. It was reported that HMGB1 with a disulfide bond between C23 and C45 mostly activates TLR4, while reduced extracellular HMGB1 binds to the RAGE receptor [31]. The higher HMGB1 level and more macrophages infiltration represented enhanced inflammatory responses in HMGB1ECKO mice post ischemic insult, and the sensitive endothelial cells might thus suffer more under excessive inflammation, which could contribute to the retarded ischemia recovery even under higher VEGF condition (Supplementary Fig. 5). Consistent with in vitro results and previous study [5], our in vivo study in the HLI model indicates intracellular HMGB1 may even outweigh the function of extracellular HMGB1, as an signaling molecule or DAMP during ischemic or inflammatory stress conditions.

One of the most well characterized endothelial dysfunction indicator is the impairment of EDR. In our study, we demonstrated that HMGB1 deletion in endothelial cells resulted in impaired EDR and hypertension in this HMGB1ECKO mice model, which may caused by reduced NO production. As a biomarker for endothelial function, NO has numerous molecular targets [32]. In physiological conditions, nitric oxide (NO) acts as a modulator of both vascular tone and structure, playing a predominant protective role on the vasculature. NO produced by eNOS can also promote cell proliferation under certain conditions [33], although the underlying mechanisms responsible for this effect are still not clear. In our study, the proliferation of HUVECs was impaired after HMGB1 knockdown by siRNA, which can be attributed to the decreased NO production in this setting. In our study, NO production was decreased in the serum from HMGB1ECKO mice, which can partly explain the hypertension and retarded blood flow recovery post hind limb ischemia in this HMGB1ECKO mice model.

In endothelial cells, NO synthesis is catalyzed from L-arginine. Through phosphorylation on Ser1177, the activity of eNOS is regulated by the serine/threonine protein kinase Akt. In this study, we confirmed the crucial role of Akt/eNOS pathway in cell and tissue level in the setting of HMGB1 deficiency. Both in HUVECs (HMGB1 siRNA knockdown) and aortas of HMGB1ECKO mice, p-Akt expression was significantly decreased while total Akt level remained unchanged. Although the mechanism for AKT inactivation regulated by HMGB1 deficiency in endothelial cells is still unclear, it is possible that DNA damage caused by HMGB1 deficiency might induce abnormal transcription and proteins translation, which leads to the inactivation of AKT pathway. Further studies are needed to verify this issue.

ROS not only plays an important role in signal transduction, but also play pivotal roles in physiological regulation of cardiovascular system through facilitating various biological responses, including senescence in heart and endothelial cells [34–37]. Endothelial dysfunction usually caused by increased intracellular ROS productions through several mechanisms such as NO inactivation, formation of peroxinitrite and NO synthase uncoupling. Our study demonstrated that HMGB1 deletion or knockdown in endothelial cells could result in increased ROS production, which is consistent with the published data [2]. Due to the enhanced oxidative stress, an increased degradation of NO might then follow. Besides, accumulation of ROS might also lead to widespread cellular damage and impaired angiogenesis. Superoxide dismutase (SOD) is one of the most efficient enzymatic antioxidants. SOD catalyses the dismutation of O2 into H2O2. Ad-SOD2 was used to treat mice with hind limb ischemia in our study. As expected, we could show the rescue role of SOD in endothelial function of HMGB1ECKO mice, indicating the central role of HMGB1 in the mediation of angiogenesis post ischemic injury.

Clinically, most clinical diseases, which were found to be relevant to HMGB1, are associated with increased HMGB1 levels [3,38]. For example, HMGB1 expression is increased in the aortic wall of patients with abdominal aortic aneurysm. Serum HMGB1 levels are found increased in patients with heart failure, acute myocardial infarction and even in patients with diabetes, cancer and lupus nephritis. Few studies found decreased HMGB1 expression, but HMGB1 protein expression was lower in the ischemic tissue of diabetic mice than in normoglycemic mice [25]. Although it is still unclear if HMGB1 expression was also decreased in tissue of diabetic patients, it is reasonable to speculate the reduced repair capacity of ischemic tissue in diabetic mice maybe caused by decreased expression of HMGB1, which provides a hint that targeting HMGB1 might be a therapeutic option to attenuate ischemia complications in diabetes. Besides, this study also hints that locally knockdown or knockout of endothelial HMGB1 might be feasible way to inhibit angiogenesis and tumor growth.

4.1. Study limitation

There are several study limitations in our experiments. Firstly, the intracellular role of HMGB1 in endothelial cells should be confirmed in future study, for example, with the application of neutralizing antibody or internalization inhibitors in current in vitro and in vivo models. Secondly, although local macrophage infiltration was tested in both WT and HMGB1ECKO mice, inflammation in vivo was not studied systematically. Lastly, impact of HGMB1 released from non-EC cells on EC function was not explored in our study.

5. Conclusion

In summary, our findings provide further evidence supporting the molecular role of HMGB1 on mediating NO production. The most important finding of the present study is that intracellular HMGB1 deficiency causes endothelial dysfunction, which can result in hypertension and retarded blood flow recovery of ischemic muscle in mouse despite higher serum HMGB1 level and HMGB1 expression in ischemic tissue. The loss of HMGB1 contributes to decreased p-Akt expression, which subsequently suppress eNOS expression and activity, on the other hand, loss of HMGB1 in endothelial cells increases ROS production, which can further decrease NO, thereby forming the vicious circle promoting the endothelial function and responsible for disturbed blood pressure regulation and blood flow recovery post ischemic insult in HMGB1ECKO mice. Mechanistically, we find that NO production in endothelial cells deficiency of HMGB1 is regulated by eNOS and ROS

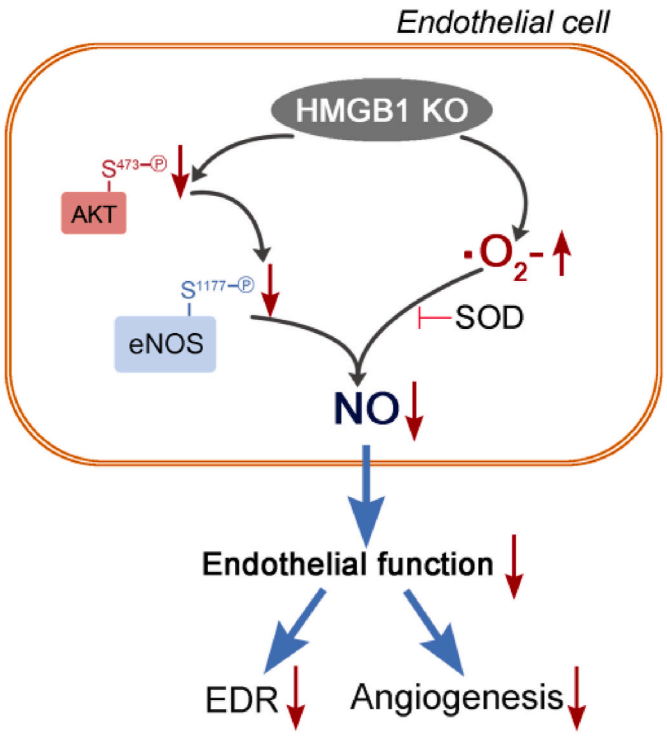

Fig. 7. Illustration of effect and possible pathway after HMGB1 loss in endothelial cells.

together (Fig. 7).

Sources of funding

This work was supported in part by the National Natural Science Foundation of China (NSFC) Projects 81600248 (to Z Zhu) and 81800414 (to Q Zhou), Natural Science Foundation of Hunan Province, China Projects 2018JJ3744 (to Z Zhu) and 2018JJ3732 (to Q Zhou).

Declaration of competing interest

There is no conflict of interest including any financial, personal or other relationships with other people or organizations within three years of beginning the submitted work that could inappropriately influence, or be perceived to influence, their work.

Acknowledgments

None.

Appendix A. Supplementary data

Supplementary data to this article can be found online at https://doi.org/10.1016/j.redox.2021.101890.

References

[1] K. Javaherian, J.F. Liu, J.C. Wang, Nonhistone proteins HMG1 and HMG2 change the DNA helical structure, Science 199 (1978) 1345–1346.
[2] M.E. Bianchi, M.P. Crippa, A.A. Manfredi, et al., High-mobility group box 1 protein orchestrates responses to tissue damage via inflammation, innate and adaptive immunity, and tissue repair, Immunol. Rev. 280 (2017) 74–82.
[3] D. Tang, R. Kang, H.J. Zeh 3rd, et al., High-mobility group box 1, oxidative stress, and disease, Antioxidants Redox Signal. 14 (2011) 1315–1335.
[4] M.S. Kwak, H.S. Kim, K. Lkhamsuren, et al., Peroxiredoxin-mediated disulfide bond formation is required for nucleocytoplasmic translocation and secretion of HMGB1 in response to inflammatory stimuli, Redox biology 24 (2019) 101203.
[5] H. Huang, G.W. Nace, K.A. McDonald, et al., Hepatocyte-specific high-mobility group box 1 deletion worsens the injury in liver ischemia/reperfusion: a role for intracellular high-mobility group box 1 in cellular protection, Hepatology 59 (2014) 1984–1997.
[6] R. Kang, Q. Zhang, W. Hou, et al., Intracellular Hmgb1 inhibits inflammatory nucleosome release and limits acute pancreatitis in mice, Gastroenterology 146 (2014) 1097–1107.
[7] H. Yanai, A. Matsuda, J. An, et al., Conditional ablation of HMGB1 in mice reveals its protective function against endotoxemia and bacterial infection, Proc. Natl. Acad. Sci. U.S.A. 110 (2013) 20699–20704.
[8] Y.G. Zhang, X. Zhu, R. Lu, et al., Intestinal epithelial HMGB1 inhibits bacterial infection via STAT3 regulation of autophagy, Autophagy 15 (2019) 1935–1953.
[9] X. Li, X. Sun, P. Carmeliet, Hallmarks of endothelial cell metabolism in health and disease, Cell Metabol. 30 (2019) 414–433.
[10] G.G. Camici, G. Savarese, A. Akhmedov, et al., Molecular mechanism of endothelial and vascular aging: implications for cardiovascular disease, Eur. Heart J. 36 (2015) 3392–3403.
[11] S. Masi, G. Georgiopoulos, M. Chiriaco, et al., The importance of endothelial dysfunction in resistance artery remodelling and cardiovascular risk, Cardiovasc. Res. 116 (2020) 429–437.
[12] Z. Ungvari, S. Tarantini, T. Kiss, et al., Endothelial dysfunction and angiogenesis impairment in the ageing vasculature, Nat. Rev. Cardiol. 15 (2018) 555–565.
[13] E. Eroglu, S.S.S. Saravi, A. Sorrentino, et al., Discordance between eNOS phosphorylation and activation revealed by multispectral imaging and chemogenetic methods, Proc. Natl. Acad. Sci. U.S.A. 116 (2019) 20210–20217.
[14] M. Schleicher, J. Yu, T. Murata, et al., The Akt1-eNOS axis illustrates the specificity of kinase-substrate relationships in vivo, Sci. Signal. 2 (2009) ra41.
[15] S. Wang, R. Chennupati, H. Kaur, et al., Endothelial cation channel PIEZO1 controls blood pressure by mediating flow-induced ATP release, J. Clin. Invest. 126 (2016) 4527–4536.
[16] E.M. Bauer, R. Shapiro, T.R. Billiar, et al., High mobility group Box 1 inhibits human pulmonary artery endothelial cell migration via a Toll-like receptor 4- and interferon response factor 3-dependent mechanism(s), J. Biol. Chem. 288 (2013) 1365–1373.
[17] S. Ghaffari, E. Jang, F.N. Nabi, et al., Endothelial HMGB1 is a critical regulator of LDL transcytosis via an SREBP2-SR-BI Axis, Arterioscler. Thromb. Vasc. Biol. 41 (1) (2021) 200–216.
[18] J. Lan, H. Luo, R. Wu, et al., Internalization of HMGB1 (high mobility group box 1) promotes angiogenesis in endothelial cells, Arterioscler. Thromb. Vasc. Biol. 40 (12) (2020) 2922–2940.
[19] Z. Zhu, X. Peng, X. Li, et al., HMGB1 impairs endothelium-dependent relaxation in diabetes through TLR4/eNOS pathway, Faseb. J.: official publication of the Federation of American Societies for Experimental Biology 34 (2020) 8641–8652.
[20] E.E. Mulvihill, E.M. Varin, J.R. Ussher, et al., Inhibition of dipeptidyl peptidase-4 impairs ventricular function and promotes cardiac fibrosis in high fat-fed diabetic mice, Diabetes 65 (2016) 742–754.
[21] Z. Zhu, X. Peng, X. Li, et al., Association between radiation exposure and endothelium-dependent vasodilation: results from clinical and experimental studies, J. Vasc. Intervent. Radiol. 31 (2020) 42–48.
[22] S. Kroller-Schon, T. Jansen, T.L.P. Tran, et al., Endothelial alpha1AMPK modulates angiotensin II-mediated vascular inflammation and dysfunction, Basic Res. Cardiol. 114 (2019) 8.
[23] M. Baker, S.D. Robinson, T. Lechertier, et al., Use of the mouse aortic ring assay to study angiogenesis, Nat. Protoc. 7 (2011) 89–104.
[24] R. Bartoszewski, A. Moszynska, M. Serocki, et al., Primary endothelial cell-specific regulation of hypoxia-inducible factor (HIF)-1 and HIF-2 and their target gene expression profiles during hypoxia, Faseb. J.: official publication of the Federation of American Societies for Experimental Biology 33 (2019) 7929–7941.
[25] F. Biscetti, G. Straface, R. De Cristofaro, et al., High-mobility group box-1 protein promotes angiogenesis after peripheral ischemia in diabetic mice through a VEGF-dependent mechanism, Diabetes 59 (2010) 1496–1505.
[26] J. Yu, E.D. deMuinck, Z. Zhuang, et al., Endothelial nitric oxide synthase is critical for ischemic remodeling, mural cell recruitment, and blood flow reserve, Proc. Natl. Acad. Sci. U.S.A. 102 (2005) 10999–11004.
[27] E. Gustafsson, C. Brakebusch, K. Hietanen, et al., Tie-1-directed expression of Cre recombinase in endothelial cells of embryoid bodies and transgenic mice, J. Cell Sci. 114 (2001) 671–676.
[28] Y.Y. Kisanuki, R.E. Hammer, J. Miyazaki, et al., Tie2-Cre transgenic mice: a new model for endothelial cell-lineage analysis in vivo, Dev. Biol. 230 (2001) 230–242.
[29] J.A. Alva, A.C. Zovein, A. Monvoisin, et al., VE-Cadherin-Cre-recombinase transgenic mouse: a tool for lineage analysis and gene deletion in endothelial cells, Developmental Dynamics: an official publication of the American Association of Anatomists 235 (2006) 759–767.
[30] Y.F. Xu, Z.L. Liu, C. Pan, et al., HMGB1 correlates with angiogenesis and poor prognosis of perihilar cholangiocarcinoma via elevating VEGFR2 of vessel endothelium, Oncogene 38 (2019) 868–880.
[31] C. Janko, M. Filipovic, L.E. Munoz, et al., Redox modulation of HMGB1-related signaling, Antioxidants Redox Signal. 20 (2014) 1075–1085.
[32] J. Tejero, S. Shiva, M.T. Gladwin, Sources of vascular nitric oxide and reactive oxygen species and their regulation, Physiol. Rev. 99 (2019) 311–379.
[33] C. Napoli, G. Paolisso, A. Casamassimi, et al., Effects of nitric oxide on cell proliferation: novel insights, J. Am. Coll. Cardiol. 62 (2013) 89–95.
[34] H. Sies, D.P. Jones, Reactive oxygen species (ROS) as pleiotropic physiological signalling agents, Nat. Rev. Mol. Cell Biol. 21 (2020) 363–383.
[35] S.J. Forrester, D.S. Kikuchi, M.S. Hernandes, et al., Reactive oxygen species in metabolic and inflammatory signaling, Circ. Res. 122 (2018) 877–902.

[36] T. Cao, S. Fan, D. Zheng, et al., Increased calpain-1 in mitochondria induces dilated heart failure in mice: role of mitochondrial superoxide anion, Basic Res. Cardiol. 114 (2019) 17.

[37] K.J. Bubb, G.R. Drummond, G.A. Figtree, New opportunities for targeting redox dysregulation in cardiovascular disease, Cardiovasc. Res. 116 (2020) 532–544.

[38] S. Yang, L. Xu, T. Yang, et al., High-mobility group box-1 and its role in angiogenesis, J. Leukoc. Biol. 95 (2014) 563–574.